HIERARCHICAL SLIDING MODE CONTROL FOR AN UNDERACTUATED MIMO SYSTEM

ĐIỀU KHIỂN TRƯỢT THỨ BẬC CHO HỆ UNDER-ACTUATED NHIỀU VÀO NHIỀU RA

[1]Nguyen Van Dong Hai, [2]Huynh Xuan Dung, [3]Nguyen Minh Tam, [3]Mircea Ivanescu, [5]Mircea Nitulescu
[1,2,3]Ho Chi Minh city University of Technology and Education (HCMUTE), Vietnam
[4,5]University of Craiova (UCV), Romania

Received 29/5/2017, Peer reviewed 24/10/2017, Accepted for publication 25/12/2017

ABSTRACT

The paper proposed a balancing control for MIMO under-actuated systems. In this paper, human walking robots, the athlete robot, are researched. The dynamic equations of this model are generated by Euler Lagrange method. The balancing control on the stance phase is studied. Balancing on one leg is a basic behavior of athlete in order to developing other behavior controlling. The hierarchical sliding mode control algorithm is proposed. Numerical simulations show the method efficiency and robustness.

Keywords: *athlete robot; balance control; Euler-Lagrange; hierarchical sliding mode control; under-actuated MIMO system.*

TÓM TẮT

Bài báo đề xuất phương pháp điều khiển cân bằng cho hệ thống under-actuated nhiều ngõ vào vào nhiều ngõ ra ra. Trong bài báo này, một hệ thống under-actuated được đưa ra làm đố tượng điều khiển là hệ robot vận động. Phương trình toán học của hệ robot trên được tính toán thông qua phương pháp Euler-Lagrange. Vấn đề điều khiển đặt ra là phải ổn định cho hệ robot đứng một chân cân bằng ở chế độ pha đứng (stance phase). Đó là một tư thế cơ bản của robot vận động trước khi phát triển các giải thuật điều khiển khác. Giải thuật điều khiển được đề nghị là điều khiển trượt thứ bậc. Các kết quả mô phỏng đã chứng minh được sự ổn định và tính bền vững của hệ thống.

Từ khóa: *robot vận động; điều khiển cân bằng; Euler-Lagrange; điều khiển trượt thứ bậc; hệ under-actuated MIMO.*

1. INTRODUCTION

The control problem of two-legged robot has focused attention of a great number of researchers during the last years. The ZMP method and the controllers for stabilizing the balance during the walking were developed in [1, 2]. A walking robot model with elastic legs for hopping and jumping were studied in [3, 4]. Ryuma Niiyama [5-7] presented the experimental results and the data processing system for a two-legged robot with elastic parts. The athlete robot (AR) as multi-input-multi-output system (MIMO) is studied in [11, 12] and [13-15]. The SIMO model is developed and the control problems of these under-actuated systems are specified.

This paper analyses the underactuated model of the AR robot (Fig 1) in the stance phase. The conditions of the balancing posture are discussed. Control algorithms are developed by using linear feedback techniques or hierarchical sliding methods.

The paper has the following structure: Section 2 analyses complete dynamic

equation of AR. Section 3 treats the control algorithm and presents the simulation results. Section 4 is dedicated to conclusion.

2. MATHEMATICAL MODELLING

2.1 Dynamic Equation

The elastic legs of a disabled people were proposed, first, by Ryuma [5-7], (Fig. 2). The two torques of a classical actuation of a walking robot are substituted by a single torque of the elastic component of the leg (Fig 3).

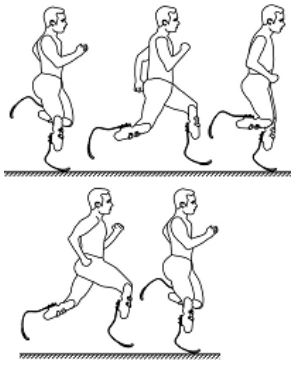

Fig. 1. *Elastic legs for disabled people [16]*

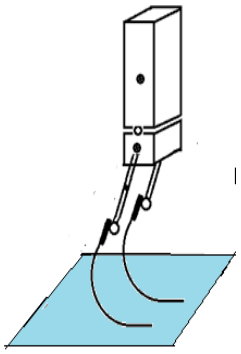

Fig. 2. *Equivalent robot*

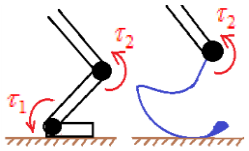

Fig. 3.

Correlation between solid leg and elastic leg

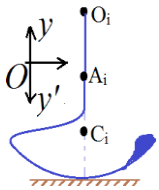

Fig. 4.

Self-balance position of elastic legs

An AR can be modeled in mathematical form in Fig. 5, including five links. The geometric characteristics are the following:

- Link 1 and link 5 are elastic round with radius r. The centers of each round of link 1 and 5 are A_1 and A_5. The contact points of link 1 and 5 to the nearest links (link 2 and 4) are O_1, O_4. Mass of link 1 and 5 are very small to mass of other links.
- Link 3 is the body of AR, with length $l_3 = 0$. Link 3 occupies almost the mass of whole robot $m_3 \gg m_i$ with $i = 1,2,4,5$
- Link 2 and 4 are solid links.
- The elastic legs are designed as in self-balance position : $A_iO_ix = A_iC_ix = \frac{\pi}{2}$ (no external forces effect) (Fig. 4).

System parameters are listed in Table I and the coordinates of important points of AR are presented in Appendix.

Table.1: *Variables and Parameters of AR*

Para-meters	Unit	Description
m_i	kg	Mass of link i $(i=1,2,3,4,5)$; $m_1 = m_5$; $m_2 = m_4$
l_i	m	Length of link i $(i=2,3,4)$; $l_2 = l_4$; $l_3 = 0$
α_1	**rad**	Angle between vertical axis with link 1 and $\alpha_1 = C_1O_1y'$
α_i	**rad**	Angle between link I with the next link $(i = 2,3,4,5)$
I_i	**kgm^2**	Inertial moment of link i
r	m	Radius of round part of link 1 and 5
k	Nm/rad	Rotational spring coefficient

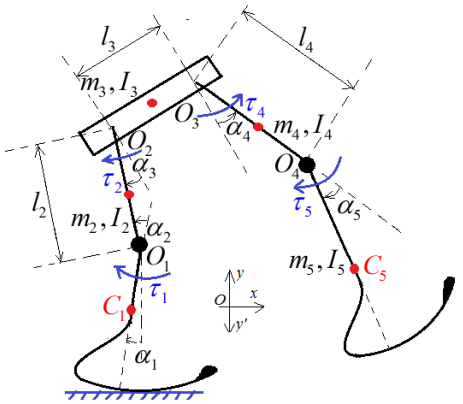

Fig. 5. *Mathematical form of AR*

Behavior of elastic leg is determined by Castigliano's Theorem [17] which provides a good tool for analyzing forces on curved components. AR can be regarded as equivalent inverted pendulum, Fig 6. Elastic legs are equivalent to springs.

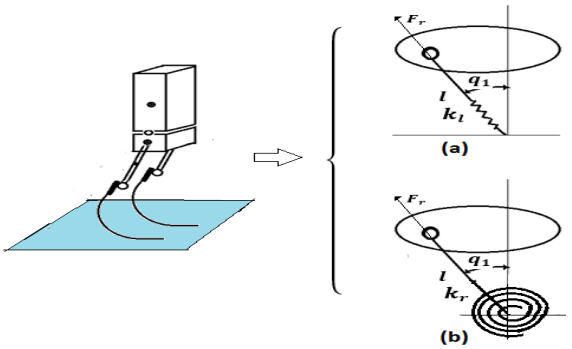

Fig. 6. *Equivalent Pendulum Model:*

a)-as linear spring b)-as rotational spring

Consider the equivalent model of Fig 6b. The elastic strain potential energy will be

$$P_{strain} = \frac{1}{2} k \alpha_1^2 \tag{1}$$

The global potential energy is:

$$P = g \sum_{i=1}^{5} m_i y_{Ci} + P_{strain} \tag{2}$$

$$K = \sum_{i=1}^{5} \left[\frac{m_i}{2} \left(\dot{x}_{Ci}^2 + \dot{y}_{Ci}^2 \right) + \frac{I_i}{2} \dot{\alpha}_i^2 \right] \tag{3}$$

By using the Lagrange operator

$$L = K - P \tag{4}$$

dynamic equations generated from Euler-Lagrange method will be

$$\frac{\partial L}{\partial \alpha_i} - \frac{d}{dt}\left(\frac{\partial L}{\partial \dot{\alpha}_i} \right) = \tau_i \quad (i = 2,3...,5) \tag{5}$$

$$\frac{\partial L}{\partial \alpha_1} - \frac{d}{dt}\left(\frac{\partial L}{\partial \dot{\alpha}_1} \right) = 0 \tag{6}$$

Equations (5) and (6) can be rewritten into matrix form:

$$J(\alpha_i)\ddot{\alpha} = F(\alpha_i, \dot{\alpha}_i) + \tau \tag{7}$$

Where:
$$\begin{cases} \alpha = [\alpha_1 \quad \alpha_2 \quad \cdots \quad \alpha_5]^T \\ \tau = [0 \quad \tau_2 \quad \tau_3 \quad \tau_4 \quad \tau_5]^T \end{cases} \tag{8}$$

The matrices J and F are so long and complicated to be listed here. But these matrices can be calculated by computer program (by MATLAB/SIMULINK).

2.2 Equivalent Model

To solve the complex model (7), an equivalent model (EM) as presented in Fig 7, 8 is proposed, where the parameters are listed in Table 2 and the angle θ^* is assumed to consist of two elements:

- The element $\theta = \alpha_2$, which is not effected by motion of links 3, 4, 5.
- The element $\Delta\theta$, which is caused by motion of links 3, 4, 5.

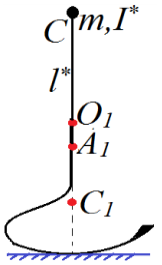

Fig.7. *Equivalent model in balance position*

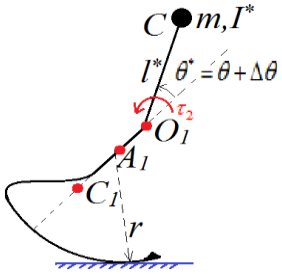

Fig. 8. *Motion of equivalent model*

Table. 2: *Variables of EM*

Parameters	Unit	Description
l^*	m	Distance from new center of the upper part (including link 2, 3, 4, 5) to the root of link 1 $(l^* = O_1C)$
I^*	kgm^2	Inertial moment of upper part (including link 2,3,4,5)
m	rad	Equivalent mass of upper part (including link 2,3,4,5)
θ^*	rad	Angle between link 1 and link 2 $(\theta^* = \theta + \Delta\theta)$

The parameters of Table II are

$$m = \sum_{i=2}^{5} m_i = const \tag{9}$$

$$l^* = \sqrt{\left(x_C - x_{O1}\right)^2 + \left(y_C - y_{O1}\right)^2} \quad (10)$$

$$I^* = m\left(l^*\right)^2 \quad (11)$$

$$\theta^* = \theta + \Delta\theta = \arctan\left(\frac{x_C - x_{O1}}{y_C - y_{O1}}\right) - \alpha_1 \quad (12)$$

The co-ordinate of center of mass C is:

$$x_C = \sum_{i=2}^{5} \frac{x_{Ci} m_i}{m_i} \quad (13)$$

$$y_C = \sum_{i=2}^{5} \frac{y_{Ci} m_i}{m_i} \quad (14)$$

The kinetic and elastic strain potential energy of EM are:

$$K = \frac{m_1}{2}\left(\dot{x}_{C1}^2 + \dot{y}_{C1}^2\right) + \frac{m}{2}\left(\dot{x}_C^2 + \dot{y}_C^2\right) + \frac{I_1}{2}\dot{\alpha}_1^2 + \frac{I}{2}\left(\dot{\theta} - \dot{\alpha}_1\right)^2 \quad (15)$$

$$P_{strain} = \frac{k}{2}\alpha_1^2 \quad (16)$$

Total potential energy will be

$$P = m_1 g y_{C1} + m g y_C + P_{strain} \quad (17)$$

By using the Lagrange operator (4), dynamic equations of EM by Euler-Lagrange method are

$$\frac{\partial L}{\partial \alpha_1} - \frac{d}{dt}\left(\frac{\partial L}{\partial \dot{\alpha}_1}\right) = 0 \quad (18)$$

$$\frac{\partial L}{\partial \theta^*} - \frac{d}{dt}\left(\frac{\partial L}{\partial \dot{\theta}^*}\right) = \tau_2 \quad (19)$$

Dynamic equation (18), (19) can be re-written into matrix form:

$$\underbrace{\begin{bmatrix} J_{11} & J_{12} \\ J_{21} & J_{22} \end{bmatrix}}_{J} \begin{bmatrix} \ddot{\alpha}_1 \\ \ddot{\theta}^* \end{bmatrix} = \underbrace{\begin{bmatrix} f_1 \\ f_2 \end{bmatrix}}_{f} + \begin{bmatrix} 0 \\ \tau_2 \end{bmatrix} \quad (20)$$

Where

$$J_{11} = 2\gamma_3 m_1 r cos\alpha_1 - I^* - \gamma_3^2 m_1 - \gamma_4^2 m - \left(l^*\right)^2 m + \\ -mr^2 - m_1 r^2 - 2\gamma_4 l^* m cos\theta^* - I_1^* - 2\gamma_4 m r cos\alpha_1 + \\ -2l^* m r cos\left(\alpha_1 - \theta^*\right) \quad (21)$$

$$J_{21} = J_{12} = I^* + \left(l^*\right)^2 m + \gamma_4 l^* m cos\theta + l^* m r cos\left(\alpha_1 - \theta^*\right) \quad (22)$$

$$J_{22} = -m\left(l^*\right)^2 - I^* \quad (23)$$

$$f_1 = k\alpha_1 + g\gamma_3 m_1 sin\alpha_1 - g\gamma_4 m sin\alpha_1 - g l^* m sin\left(\alpha_1 - \theta^*\right) + \\ -\gamma_3 m_1 \dot{\alpha}_1^2 r sin\alpha_1 + \gamma_4 m \dot{\alpha}_1^2 r sin\alpha_1 + l^* m \dot{\alpha}_1^2 r sin\left(\alpha_1 - \theta^*\right) + \\ -l^* m \dot{\alpha}_1 r \dot{\theta}^* sin\left(\alpha_1 - \theta^*\right) \quad (24)$$

$$f_2 = l^* m \begin{bmatrix} g sin\left(\alpha_1 - \theta^*\right) + \gamma_4 \dot{\alpha}_1^2 sin\theta^* - \dot{\alpha}_1^2 r sin\left(\alpha_1 - \theta^*\right) + \\ -\gamma_4 \dot{\alpha}_1 \dot{\theta}^* sin\theta^* + \dot{\alpha}_1 r \dot{\theta}^* sin\left(\alpha_1 - \theta^*\right) \end{bmatrix} \quad (25)$$

The effects of motion of upper part can be decreased if the following conditions are satisfied:

- Length of link 2 is small.
- Mass of link 3 is much bigger than mass of other links
- Link 2, 3, 4, 5 are controlled in good set-point positions.

Depending on these conditions, two basic different cases are listed below.

- Case 1: system parameters are:

$$\gamma_1 = 0.1(m);\ \gamma_2 = 0.2(m);\ r = 0.4(m);\ \gamma_3 = r - \gamma_1; \\ \gamma_4 = \gamma_2 - r;\ m_1 = 0.001(kg);\ m_2 = 0.01(kg); \\ m_3 = 0.7(kg);\ I_1 = 0.001(kgm^2);\ I_2 = 0.01(kgm^2); \\ I_3 = 0.1(kgm^2);\ l_3 = 0(m);\ l_2 = 0.2(m); \\ g = 9.81\left(N/kgm^2\right);\ k = 0.2\left(N/kgm^2\right). \quad (26)$$

In this case, ranging of equivalent parameters of EM is:

$$0.0279(kgm^2) \le I \le 0.0282(kgm^2); \\ 0.1965(m) \le l \le 0.1978(m); \\ -0.009(rad) \le \Delta\theta \le 0.009(rad) \quad (27)$$

- Case 2: : system parameters are:

$$\gamma_1 = 0.1(m);\ \gamma_2 = 0.2(m);\ r = 0.4(m);\ \gamma_3 = r - \gamma_1; \\ \gamma_4 = \gamma_2 - r;\ m_1 = 0.01(kg);\ m_2 = 0.1(kg);\ m_3 = 0.5(kg); \\ I_1 = 0.001(kgm^2);\ I_2 = 0.02(kgm^2);\ I_3 = 0.1(kgm^2); \\ l_3 = 0(m);\ l_2 = 0.2(m);\ g = 9.81\left(N/kgm^2\right) \quad (28)$$

In this case, from (9)-(11), ranges of equivalent parameters of EM are:

$$0.019(kgm^2) \le I \le 0.031(kgm^2);\ 0.165(m) \le l \le 0.210(m); \\ -0.17(rad) \le \Delta\theta \le 0.17(rad) \quad (29)$$

3. CONTROLLER DESIGN

3.1 Linear Feedback Control

Consider a linear LQR control [9] and the linearized model of (20), defined around the point q_0

$$\dot{q} = Aq + B\tau_2 \tag{30}$$

where: $q = \begin{bmatrix} \alpha_1 & \dot{\alpha}_1 & \theta^* & \dot{\theta}^* \end{bmatrix}^T$ (31)

At the selected reference point (Fig 7), $q_0 = \begin{bmatrix} 0 & 0 & 0 & 0 \end{bmatrix}^T$, the system is proved to be controllable.

The weighted matrix is chosen as unit matrix

$$Q = diag(5,5); \quad R = 1 \tag{32}$$

The control law is selected as

$$\tau_2 = K_1\alpha_1 + K_2\dot{\alpha}_1 + K_3\theta_1^* + K_4\dot{\theta}_1^* \tag{33}$$

Where $K = \begin{bmatrix} K_1 & K_2 & K_3 & K_4 \end{bmatrix}$ is obtained by associated Ricatti equation.

Case 1:

From (26), (30), (32), feedback control matrix is calculated as: $K = \begin{bmatrix} 1.7829 & 0.7094 & -3.9039 & -0.9368 \end{bmatrix}$

Responses of EM are shown in Fig. 9, 10

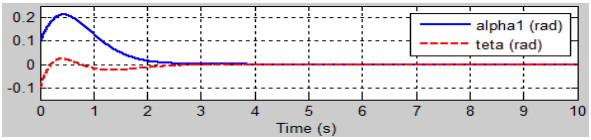

Fig. 9. *Trajectories of α_1 and θ with no effect from motion of upper part $(\Delta\theta = 0)$*

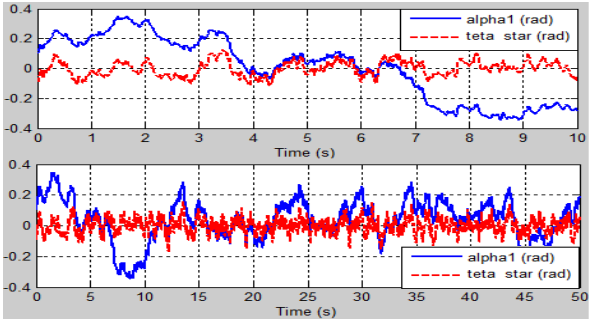

Fig. 10. *Trajectories of α_1 and θ^* for the random effect of upper part from time 0s to 10s and from time 0s to 50s*

Case 2:

From (28), (30), (32), feedback control matrix is calculated:

$$K = \begin{bmatrix} 1.5223 & 0.6210 & -3.5961 & -0.8557 \end{bmatrix}$$

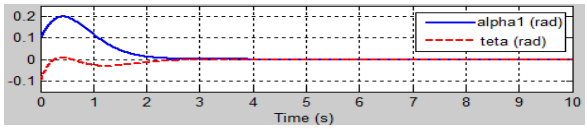

Fig. 11. *Trajectories of α_1 and θ with no effect from motion of upper part $(\Delta\theta = 0)$*

Fig. 11 shows good response when there is no-effect of upper part. But, with the motion of upper part, LQR controller cannot stabilized the system. Therefore, we remark that the quality of motion is not sufficiently good.

3.2 Sliding Mode Control

The dynamic model (20) can be re-written as:

$$\begin{cases} \ddot{\alpha} = f_1^* + b_1^*\tau_2 \\ \ddot{\theta}^* = f_2^* + b_2^*\tau_2 \end{cases} \tag{33}$$

Based on [10], process of designing hierarchical sliding control is introduced from (34) -(43) as

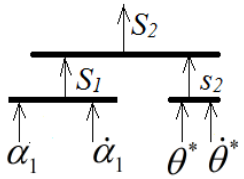

Fig. 12. *Hierarchical sliding surfaces structure for system which has one control input and four output variables*

Sliding surfaces are

$$s_1 = c_1\alpha_1 + \dot{\alpha}_1 \tag{34}$$

$$s_2 = c_2\theta^* + \dot{\theta}^* \tag{35}$$

Where: $c_1, c_2 > 0$ (36)

The derivative with respect time of (34), (35) yields

$$\dot{s}_1 = c_1\dot{\alpha}_1 + f_1^* + b_1^*\tau_2 \tag{37}$$

$$\dot{s}_2 = c_2\dot{\theta}^* + f_2^* + b_2^*\tau_2 \tag{38}$$

The equivalent controls are

$$u_{eq1} = -\left(c_1\dot{\alpha}_1 + f_1^*\right)/b_1^* \quad (39)$$

$$u_{eq2} = -\left(c_2\dot{\theta}^* + f_2^*\right)/b_2^* \quad (40)$$

Define

$$S_1 = a_1 s_1 \quad (41)$$

$$S_2 = a_2 s_2 + s_1 \quad (42)$$

Hierarchical control law is inferred [10] as

$$\tau_2 = \frac{(a_1a_2)b_1u_{eq1} + (a_2)b_1u_{eq2} - (k_2S_2 + \eta_2 \operatorname{sgn} S_2)}{(a_1a_2)b_1 + (a_2)b_1} \quad (43)$$

In order to obtain a good quality of motion, the control parameters are selected by genetic algorithms as

$$a_1 = 0.01 \;;\; a_2 = 2.42 \;;\; c_1 = 5.94 \;;\; c_2 = 1.04 \;;$$
$$k_2 = 7.96 \;;\; \eta_2 = 2.8 \quad (44)$$

Case 1: Responses of EM from the parameters (43) are shown in Fig. 13, 14

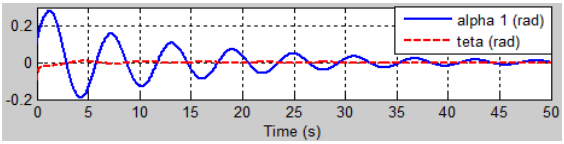

Fig. 13. *Trajectories of α_1 and θ^* with no effect from motion of upper part $(\Delta\theta = 0)$*

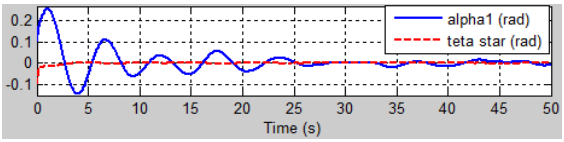

Fig. 14. *Trajectories of α_1 and θ^* for the random effect of upper part from time 0s to 50s*

Fig 13, 14 show the good quality of the sliding control comparative with LQR control.

Case 2: Responses of EM from the parameters (43) are shown in Fig. 15-18

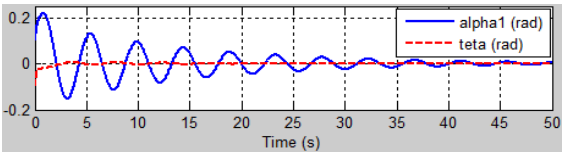

Fig. 15. *Trajectories of α_1 and θ with no effect from motion of upper part $(\Delta\theta = 0)$*

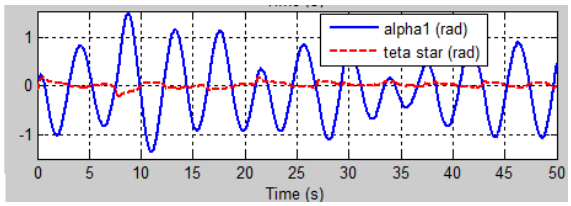

Fig. 16. *Trajectories of α_1 and θ^* for the random effect of upper part from time 0s to 10s and from 0s to 50s*

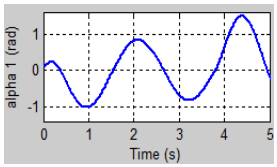

Fig. 17. *Trajectory of α_1 for the random effect of upper part from time 0s to 5s*

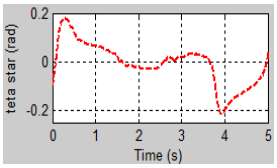

Fig. 18. *Trajectory of θ^* for the random effect of upper part from time 0s to 5s*

3.3. Mixed Controller for Balancing

Define: $e_i = \alpha_i - \alpha_{id}$ with $(i = 1,2,...5)$ (45)

where: $\alpha = \begin{bmatrix}\alpha_1 & \alpha_2 & \cdots & \alpha_5\end{bmatrix}^T$ (46)

$$\alpha_d = \begin{bmatrix}\alpha_{1d} & \alpha_{2d} & \cdots & \alpha_{5d}\end{bmatrix}^T \quad (47)$$

$$e = \begin{bmatrix}e_1 & e_2 & \cdots & e_5\end{bmatrix}^T \quad (48)$$

Dynamic equation from (7) can be re-written as:

$$\ddot{\alpha} = J^{-1}F + J^{-1}\begin{bmatrix}0 & 0 & \tau_3 & \tau_4 & \tau_5\end{bmatrix}^T + \\ + J^{-1}\begin{bmatrix}0 & \tau_2 & 0 & 0 & 0\end{bmatrix}^T \quad (49)$$

A proportional controller for link 3, 4, 5, is proposed

$$\tau_i = K_{pi}e_i \quad (i = 3,4,5) \quad (50)$$

Assume that $\alpha_d = const$ (51)

$$\rightarrow \quad \dot{\alpha}_d = \ddot{\alpha}_d = 0 \quad (52)$$

Also, define:

$$f^* = \begin{bmatrix} f_1^* & f_2^* & \cdots & f_5^*\end{bmatrix}^T$$
$$= \begin{bmatrix} f_1^*(e,\dot{e}) & f_2^*(e,\dot{e}) & \cdots & f_5^*(e,\dot{e})\end{bmatrix}^T \quad (53)$$
$$= J^{-1}F + J^{-1}\begin{bmatrix}0 & 0 & \tau_3 & \tau_4 & \tau_5\end{bmatrix}^T + \ddot{\alpha}_d$$

Substitute (52) into (53), yields

$$f^* = J^{-1}F + J^{-1}\begin{bmatrix}0 & 0 & \tau_3 & \tau_4 & \tau_5\end{bmatrix}^T \quad (54)$$

Define

$$b^* = \begin{bmatrix}b_1^* & b_2^* & \cdots & b_5^*\end{bmatrix}^T = \begin{bmatrix}b_1^*(e,\dot{e}) & b_2^*(e,\dot{e}) & \cdots & b_5^*(e,\dot{e})\end{bmatrix}^T \quad (55)$$

where b^* is second column of matrix J^{-1}. From (49)-(55), system structure will be:

$$\ddot{e}_i = f_i^* + b_i^*\tau_2 \quad (i = 1,2,\ldots,5) \quad (56)$$

Structure of hierarchical sliding surfaces is shown in Fig. 19:

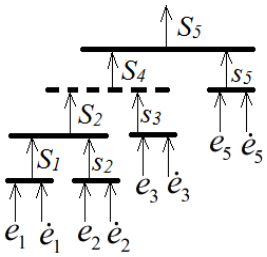

Fig. 19. *Hierarchical sliding surfaces structure for system which has one control input and five output variables*

$$s_i = c_i e_i + \dot{e}_i \quad (i = 1,2,...5) \quad (57)$$

Hierarchical control law is inferred as:

$$u_{eqi} = -\frac{c_i\dot{e}_i + f_i^*}{b_i^*} \quad (58)$$

Then, hierarchical sliding surfaces are obtained:

$$S_n = \sum_{r=1}^{n}\left(\prod_{j=r}^{n} a_j\right)s_r \quad (i = 1,2,...5) \quad (59)$$

Final control law for controller is

$$\tau_2 = \frac{\sum_{r=1}^{5}\left(\prod_{j=r}^{5} a_j\right)b_r u_{eqr} - \left(k_5 S_5 + \eta_5 \operatorname{sgn} S_5\right)}{\sum_{r=1}^{5}\left(\prod_{j=r}^{5} a_j\right)b_r} \quad (60)$$

The control parameters are selected by genetic algorithms as:

$$a_1 = 0.04;\ a_2 = 8.06;\ a_3 = 6.01;\ a_4 = 2.14;$$
$$a_5 = 5.83;\ c_1 = 5.85;\ c_2 = 5.85;\ c_3 = 6.37;$$
$$c_4 = 2.28;\ c_5 = 3.22 \quad (61)$$

$$K_{p1} = 41.44;\ K_{p2} = 39;\ K_{p3} = 22.74 \quad (62)$$

The references of balancing position are chosen as:

$$\alpha_d = \begin{bmatrix}0 & 0 & 0 & 0.1 & 0.3\end{bmatrix}^T \quad (63)$$

Case 1: With control parameters in (61), (62), system parameters in (26), (27)

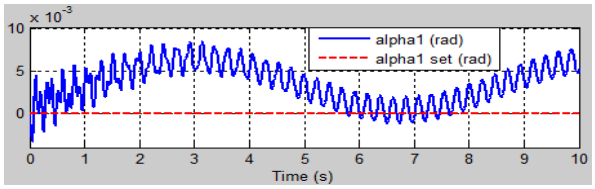

Fig. 20. *Response of Link 1*

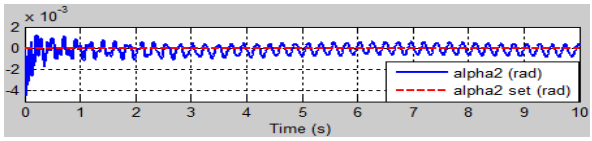

Fig. 21. *Response of Link 2*

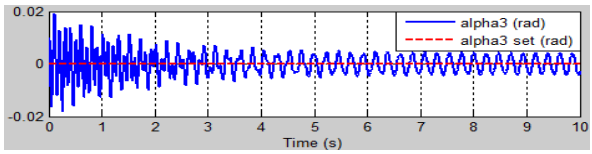

Fig. 22. *Response of Link 3*

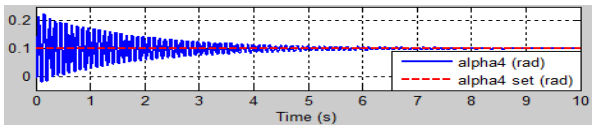

Fig.23. *Response of Link 4*

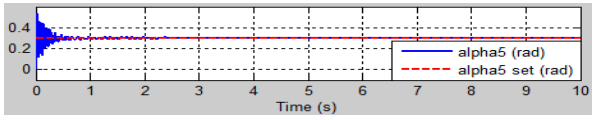

Fig. 24. *Response of Link 5*

Case 2: With control parameters in (61), (62), system parameters in (28), (29)

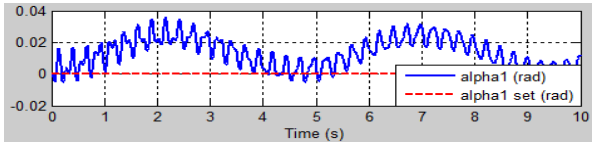

Fig. 25. *Response of Link 1*

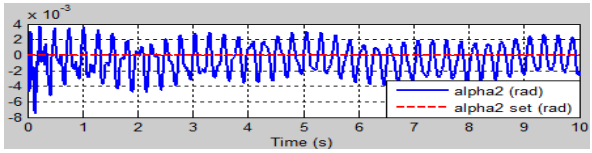

Fig. 26. *Response of Link 2*

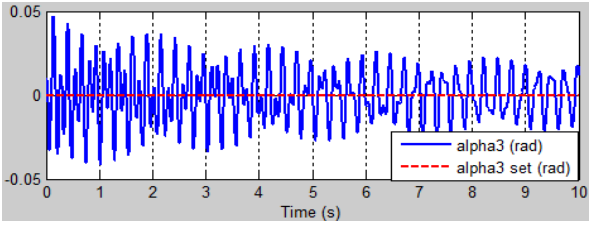

Fig. 27. *Response of Link 3*

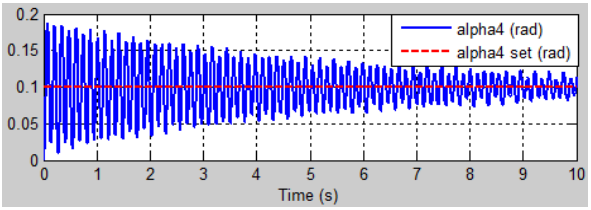

Fig. 28. Response of Link 4

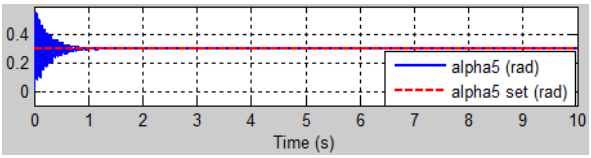

Fig. 29. *Response of Link 5*

From Fig. 20-29, the simulation results show that transformation from MIMO system to SIMO makes the system balanced in operating position. The robustness of hierarchical algorithm is guaranteed by [10]. Although settling time is still long, the responses can be improved by better solution for control parameters by searching algorithm.

4. CONCLUSION

In the paper, authors generalized the dynamic equation of AR through Euler-Lagrange. Then, this model was used to implement linear and hierarchical sliding control. The simulation results proved the robustness of sliding control. Moreover, based on the mathematical calculation in dynamic equation, the hierarchical sliding control was developed to implement an under-actuated MIMO system. All simulation results confirm that.

REFERENCES

[1] Kemalettin Erbatur, Okan Kurt, *Human Walking Robot Control with Natural ZMP References*, IEEE Annual Conference on Industrial Electronics, IECON, 2006.

[2] Zhangguo Yu, Maoxing Zheng, Qinqin Zhou, Xuechao Chen, Libo Meng, Weimin Zhang, Aiguo Ming, Qiang Hiang, *Disturbances Rejection Controller for Biped Walking Using Real-Time ZMP Regulation*, pp. 179-188, ROMANSY 21 – Robot Design, Dynamics and Control, Springer, 2016.

[3] S. H. Hyon, T. Emura, T. Mita, *Dynamics-based control of a one-legged hopping robot*, Part I: System and Control Engineering, Proceeding of International Mechanical Engineering, pp. 83-98, Vol. 217, Japan, 2003.

[4] Guang-Ping He, Xiao-Lan Tan, Xiang-Hui Zhang, Zhen Lu, *Modeling, motion planning, and control of one-legged hopping robo actuated by two arms*, Mechanism and Machine Theory, Vol. 43, Issue. 1, pp. 33-49. ScienceDirect, 2007.

[5] Ryuma Niiyama, Satoshi Nishikawa, Yasuo Kuniyoshi, *Biomechanical Approach to Open-Loop Bipedal Running with a Musculoskeletal Athlete Robot*, Journal of Advanced Robotics, Vol. 26, Issue. 3-4, 2012.

[6] Ryuma Niiyama and Yasuo Kuniyoshi, *Design of a Musculoskeletal Athlete Robot: A Biomachanical Approach*, Proceedings of the Twelfth International Conference on Climbing and Walking Robots and the Support Technologies for Mobile Machines, Turkey, 2009.

[7] http://spectrum.ieee.org/automaton/robotics/humanoids/athlete-robot-learning-to-run-like-human

[8] M. W. Spong, *The swing up control problem for Acrobot*, Journal of IEEE Control Systems, pp. 49-55, Vol. 15, Issue. 1, 1995.

[9] Brian. D. O. Anderson, John. B. Moore, *Optimal Control- Linear Quadratic Methods*, ISBN 0-13-638651-2, Prentice-Hall International, Inc, 1989.

[10] [10] Dianwei Qian, Jianqiang Yi, Dongbin Zhao, *Hierarchical Sliding Mode Control for a Class of SIMO under-actuated system*, Journal of Control and Cybernetics, Vol. 37, pp. 159-175, 2008.
[11] S. Cherdchoosilpa, S. Kuntanapreeda, N. Chaiyaratana, *MIMO controller design for a parallel manipulator system: a practitioner's approach*, IEEE ICTC '02 International Conference on Industrial Technology, 2002.
[12] Fatima Zahra Baghli, Larbi El Bakkali, Yassine Lakhal, *Multi-input Multioutput Fuzzy Logic Controller for Complex System: Application on Two-Links Manipulator*, pp. 607-614, 8th International Conference Interdisciplinarity in Engineering, Elsevier Publisher, Romania, 2014.
[13] S. Omatu, T. Fujinka, Y. Kishida, m. Yoshioka, *Self-tuning neuro-PID for SIMO systems*, European Conference on Control (ECC), Germany, 1999.
[14] Gopikrishnan. S, Ameya Anil Kesarkar, N. Selvaganesan, *Design of fractional controller for cart-pendulum SIMO system*, IEEE International Conference on Advanced Communication Control and Computing Technologies (ICACCCT), India, 2012.
[15] Chris Bowden, William Holderbaum, Victor Becerra, *Actuator placement in the multi-link inverted pendulum*, UKACC International Conference on Control, 2010.
[16] Peter G. Weiand, Matthew W. Bundle, Craig P. McGowan, Alena Grabowski, Mary Beth Brown, Rodger Kram, and Hugh Herr, *The fastest runner on artificial leg: different limbs, similar fucntion*, Journal of Applied Physiology, Vol. 107, No. 3, pp. 903-911, 2009. DOI: 10.1152/japplphysiol.00174.2009.
[17] Alberto Castigliano, *Elastic Stresses in Structures: Translated from Castigliano's Theorem de l'equibre des systemes elastiques et ses applications*, ISBN 13: 9781108070263, Cambridge University Press, 2014.

APPENDIX:

Co-ordinate of important points and links of AR in Fig. 5 are listed below:

$\gamma_3 = r - \gamma_1$; $\gamma_4 = \gamma_2 - r$; $x_{C1\_0} = 0$; $y_{C1\_0} = \gamma_1$;

$x_{A1\_0} = 0$; $y_{A1\_0} = r$; $x_{O1\_0} = 0$; $y_{O1\_0} = \gamma_2$;

$x_{A1} = x_{A1\_0} + r\alpha_1$; $y_{A1} = r$; $x_{C1} = x_{A1} - \gamma_3 \sin\alpha_1$;

$y_{C1} = y_{A1} - \gamma_3 \cos\alpha_1$; $x_{O1} = x_{A1} + \gamma_4 \sin\alpha_1$;

$y_{O1} = y_{A1} + \gamma_4 \cos\alpha_1$; $x_{O2} = x_{O1} - l_2 \sin(\alpha_2 - \alpha_1)$;

$y_{O2} = y_{O1} + l_2 \cos(\alpha_2 - \alpha_1)$; $x_{C2} = x_{O1} - l_2 \sin(\alpha_2 - \alpha_1)/2$;

$y_{C2} = y_{O1} + l_2 \cos(\alpha_2 - \alpha_1)/2$; $O_3O_2x = \alpha_3 + \alpha_2 - \alpha_1$;

$O_4O_3y' = \alpha_4 + \alpha_3 + \alpha_2 - \alpha_1$; $C_5O_4y' = O_4O_3y' - \alpha_5$;

$x_{O3} = x_{O2} + l_3 \cos O_3O_2x$; $y_{O3} = y_{O2} + l_3 \sin O_3O_2x$;

$x_{O4} = x_{O3} + l_2 \cos O_4O_3y'$; $y_{O4} = y_{O3} - l_2 \cos O_4O_3y'$;

$x_{C3} = (x_{O2} + x_{O3})/2$; $y_{C3} = (y_{O2} + y_{O3})/2$;

$x_{C4} = (x_{O3} + x_{O4})/2$; $y_{C4} = (y_{O3} + y_{O4})/2$;

$x_{C5} = x_{O4} + (\gamma_1 + \gamma_2)\sin C_5O_4y'$; $y_{C5} = y_{O4} - (\gamma_1 + \gamma_2)\sin C_5O_4y'$

Corresponding author:
Nguyen Van Dong Hai
Ho Chi Minh City University of Technology and Education, Vietnam
Email: hainvd@hcmute.edu.vn